TWIN-DISC ASSESSMENT OF THE EFFECT OF TOP-OF-RAIL FRICTION MODIFIERS ON THE TRIBOLOGICAL RESPONSE OF ER8-R370HT PAIRS FOR USE IN WHEEL-RAIL SYSTEMS

Juan C. Sánchez[1], Jaime A. Jaramillo[1], Juan F. Santa[1,2], Alejandro Toro[1]*

1: Tribology and Surfaces Group, Universidad Nacional de Colombia, Medellín, Colombia. 2: Grupo de Investigación Materiales Avanzados y Energía MATyER, Instituto Tecnológico Metropolitano, Medellín, Colombia.

**e-mail: jcsanchego@unal.edu.co*

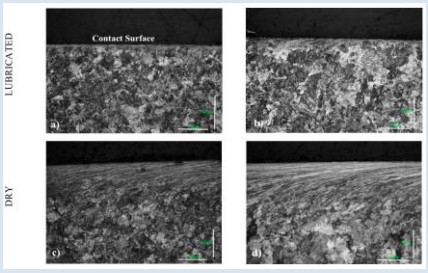

ABSTRACT

This paper studies the effect of the addition of top of rail - friction modifiers (TOR-FM's) on the tribological response of a rolling-sliding pair submitted to similar conditions to those found in commercial wheel-rail systems. The tests were conducted in a wheel-rail contact simulator (twin-disc machine) and the samples were extracted from worn wheels and rails provided by Metro de Medellín (Colombia). The tests were carried out using two Friction Modifiers. Dry tests were also performed for reference purposes. TOR-FM1 was a commercial friction modifier and TOR-FM2 was developed in the laboratory for the operating conditions of Metro de Medellín. The Hertzian contact pressure was 1 GPa and the average roughness (Ra) before the tests was fixed at 1.3 µm. The addition of friction modifiers at the interface reduced the Coefficient of Friction (COF) when compared to the dry condition, improved the surface quality and reduced the depth of the deformed material layer under the contact surface.

Keywords: Top-of-Rail Friction Modifiers, Wheel-rail contact, Wear rate, Creepage.

EVALUACIÓN MEDIANTE ENSAYOS DISCO-DISCO DEL EFECTO DE LA ADICIÓN DE MODIFICADORES DE FRICCIÓN SOBRE LA RESPUESTA TRIBOLÓGICA DE UN PAR ER8-R370HT PARA USO EN SISTEMAS RUEDA-RIEL

RESUMEN

El presente trabajo estudia el efecto de la adición de modificadores de fricción para uso en la cabeza del riel (TOR-FM's) sobre la respuesta tribológica de un par rodante-deslizante sometido a condiciones similares a las encontradas en sistemas ferroviarios comerciales. Los ensayos fueron llevados a cabo en un simulador rueda-riel tipo disco-disco y las probetas fueron extraídas de ruedas desgastadas y rieles proporcionados por el Metro de Medellín (Colombia). Los ensayos fueron realizados con dos tipos de modificadores de fricción y se estudió también la condición en seco como referencia. El TOR-FM1 fue un modificador de fricción comercial y el TOR-FM2 fue desarrollado in laboratorio para condiciones de operación del Metro de Medellín. La presión de contacto Hertziana fue de 1GPa y la rugosidad promedio (Ra) inicial fue fijada en un valor de 1.3 µm para todos los ensayos realizados. Se pudo encontrar que la adición de modificadores de fricción en la intercara favorece la reducción del coeficiente de fricción (COF) comparado con las condiciones en seco, mejora la calidad superficial y reduce la profundidad de la capa de material deformado bajo la superficie de contacto.

Palabras Claves: Modificadores de fricción TOR, Contacto rueda-riel, Tasa de desgaste, Porcentaje de deslizamiento.

Recibido: 02-03-2018 ; **Revisado:** 25-06-2018

Aceptado: 04-10-2018 ; **Publicado:** 03-01-2019

DOI: *10.5281/zenodo.7693755*

1. INTRODUCTION

The use of lubricants in a rail–wheel interface improves the performance of railway systems concerning wear and noise [1]. Over the years, the maintenance cost of railway systems has significantly increased due to wear of rails and wheels. In 1980, the United States of America (USA) spent US$ 600 million per year in rail changes [2], the European Union reported 300 million euros for the rail maintenance [3] and in 2002, the USA reported 2 billion dollars in maintenance expenses [4]. Ready et al [5] showed that maintenance expenses are higher for non-lubricated curves when compared to lubricated curves since the use of the lubricants with constant or intermittent application in the contact area leads to effective reductions in maintenance expenses.

Friction and wear control is achieved in the field by the application of a third material at the rail/wheel contact zone. The application of lubricants is done at the gauge face (GF) in the wheel flange contact, while friction modifiers (FM) are used in the top of the rail (TOR) to reduce squealing noise and surface damage related to corrugation, rolling contact fatigue and wear [6]. The application of TOR-FM also allows reducing and optimizing the level of Coefficient of Friction (COF) to keep safe operation conditions [6]. Ready et al [5] showed that the addition of a third material to the contact zone in the wheel-rail contact leads to wear rate reduction particularly in tight curves. For instance, in curves with curvature radius smaller than 200 m the wear rate is reduced up to five times. Comparable results were shown by Tameoka et al [7] who studied the difference between tests under dry conditions and with addition of TOR-FM's and greases. The authors found that the COF strongly depends on the lubrication conditions, and specifically, that the addition of a TOR-FM keeps the COF constant while lubricants and greases invariably lead to progressive reductions in friction to values low enough to prevent safe and efficient operation of railway systems during braking and traction [8].

On the other hand, when the creepage in the rail/wheel contact interface increases, the frictional force also increases. In rolling-sliding contact, there are two zones in the contact area: the adhesion zone (stick) and the slip zone. In the stick zone the velocity of the two surfaces is very similar (typical of pure rolling) but as creepage increases a new zone (slip zone) appears where there is a significant difference between the speed of the surfaces of each body in contact. When the creepage increases, the stick zone reduces and finally, the contact behaves theoretically as pure sliding [9].

In practical terms, the most important rail wear mechanism in the field is controlled abrasion generated by rail grinding. However, the fatigue life of rails is highly dependent on the COF as can be explained by the shakedown diagram [10]. If the creepage and the COF are controlled, the emergence of initial cracks can be significantly delayed [6]. Accordingly, if the COF is controlled by the addition of a TOR-FM, the surface damage can be hindered as well as the wear rate induced by rail grinding.

The variation of COF under different values of creepage when a FM is added to the contact surfaces, as well as the saturation value when the COF achieve a value similar to the 100% sliding test, constitute key information before testing the rails and wheels in the field, since the COF between rail and wheel affects the surface damage and the amount of plastic deformation at the sub-surface.

In this work, twin-disc tests were performed to determine the tribological behavior of wheel and rail materials as a function of the creepage. The tests were performed in the presence of friction modifiers and the results were compared to those obtained under dry condition. After the tests the mass losses were determined, and all the samples were submitted to worn surface inspection, microstructural analysis of the deformed layer and microhardness tests.

2. EXPERIMENTAL PROCEDURE

2.1 Samples

All the samples were extracted from wheels and rails provided by Metro Medellin. Rail samples were extracted from the head of the rail and for the wheel samples a region close to the contact band was targeted. Figure 1 shows the description of the extraction zones and the samples' size and shape. Table 1 shows the chemical composition of rail and wheel materials and Figure 2 shows the microstructure of the samples. The rail material is classified as hardened R370HT rail steel according to UNE-EN 13674 standard [11] and the wheel material as ER8 wheel steel according to UNE-EN

13262 standard [12]. The microstructure was analyzed using Scanning Electron Microscope (SEM) JEOL 5910LV and Light Optical Microscope (LOM) Nikon Eclipse Ci-L/S. The samples were polished using a standard procedure described in ASTM E3 standard and etched using Nital 2%.

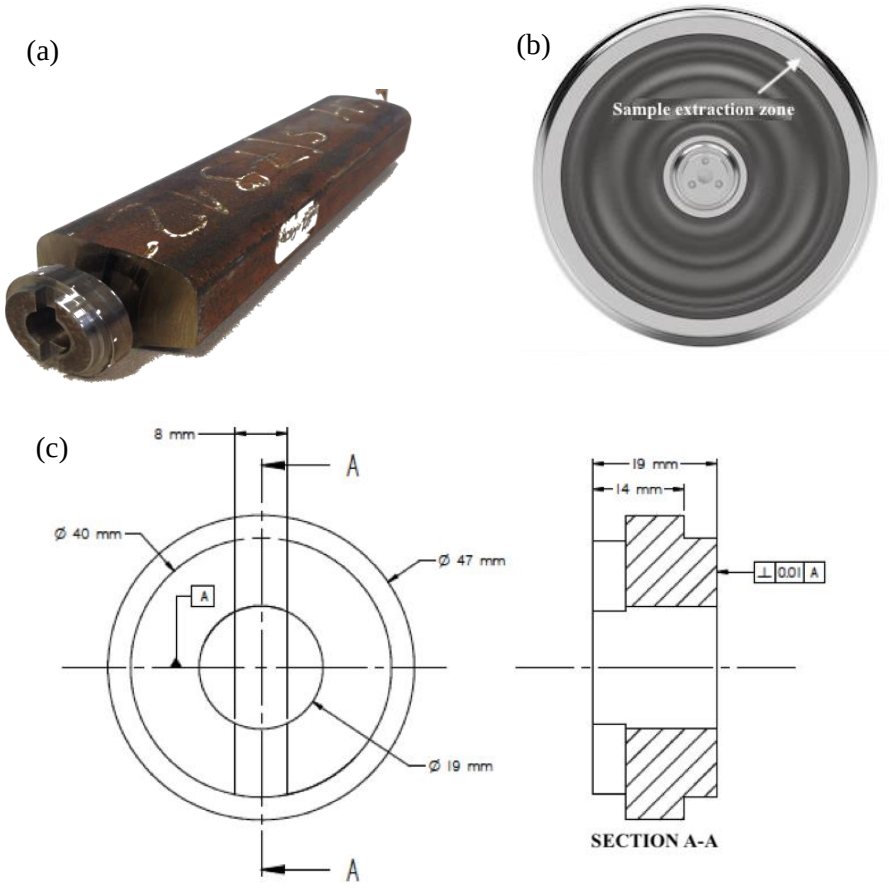

Figure 1. Zones of extraction of the samples from rails and wheels for twin-disc tests (a, b) and shape and dimensions of the samples (c).

Table 1. Chemical composition of rail and wheel materials measured by Optical Emission Spectrometry (BRUKER Q8 MAGELLAN). All the measurements were performed on surfaces polished with emery paper n. ASTM 600 with no chemical etching.

Element (wt. -%)	C	Si	Mn	S	P	Ni	Cr	Mo	Cu
Rail	0.772	0.454	1.213	0.016	0.015	0.020	0.082	0.015	0.019
Wheel	0.540	0.232	0.745	0.004	0.014	0.114	0.172	0.050	0.225

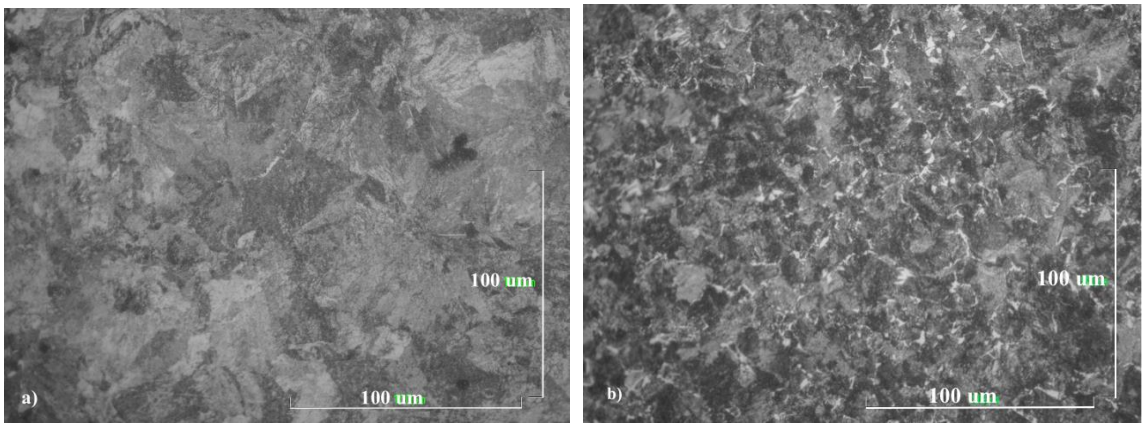

Figure 2. Microstructure of a) Rail sample (pearlite) and b) Wheel sample (pearlite + 7% ferrite).

The surface of the samples was prepared with similar processes to those used in the Metro de Medellín for maintenance purposes. The wheel samples were lathe turned whereas for the rail samples a grinding setup was used. The initial Ra of the samples (Ra = 1.3 µm) was fixed for all the experiments by controlling either the lathe turning conditions (wheel specimens) or the grinding setup parameters (rail specimens). Rz roughness parameter was also measured at the beginning of the tests and the value obtained is presented in Table 2 for both wheel and rail samples. The roughness measurements were performed with a Mitutoyo Surftest SV 3000 station profilometer.

Table 2. Roughness parameters of the samples before the tribological tests.

Sample	Ra (µm)	Rz (µm)
Rail	1.3	3.6
Wheel	1.3	1.9

2.2 Friction Modifiers physical properties

Figure 3 shows the viscosity and shear stress properties of the TOR-FM's used in the tests as a function of the shear rate.

Both friction modifiers used in this work are composed of an oil base, thickeners and solid lubricants. In the case of TOR-FM1 the base is an Ester while in TOR-FM2 it is a vegetable oil. The viscosity and shear stress of the two friction modifiers are shown in Figure 3 as a function of the shear rate. The response at low shear rates is very similar for both TOR-FM's while for high shear rates the shear stress of TOR-FM2 is lower than that of TOR-FM1.

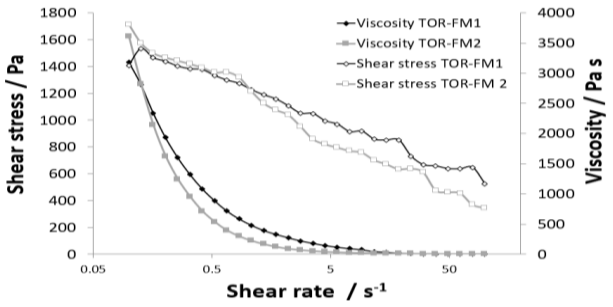

Figure 3. Viscosity and shear stress as a function of shear rate for the friction modifiers studied in this work.

2.3 Tribological tests

All the tests were carried out in a twin-disc testing machine shown schematically in Figure 4. The wheel and rail samples are mounted in two parallel shafts driven by independent electrical motors to induce and control the proper creepage during the tests. A hydraulic actuator applies the normal load to the samples and a torque transducer is used to measure the friction force generated at the contact surface. The tests were carried out under dry and lubricated conditions. For lubricated tests, two TOR-FM's were used (TOR-FM1 and TOR-FM2), being one of them (TOR-FM2) specifically developed for the operating conditions of Metro de Medellín [14]. The contact pressure used was 1 GPa and the values of creepage were selected to obtain a complete creep curve to understand the behavior of the friction modifiers under different conditions. Curves with different creepages (0.8, 3, 5 and 7%) were obtained and the COF was measured. All the tests were carried out up to 6500 cycles. A different

pair of samples (rail and wheel) was used for each tribological test and three replicas were obtained for each testing condition, i.e. Dry, TOR-FM1 and TOR-FM2.

In lubricated tests, the addition of the TOR-FM only started after initial 500 dry cycles (running-in stage). 0.05 g to 0.07 g of TOR-FM were manually added to the contact area every 500 cycles with the aid of a brush. The same method has been used previously with success to study the effect of FM's on Rolling Contact Fatigue [11, 15].

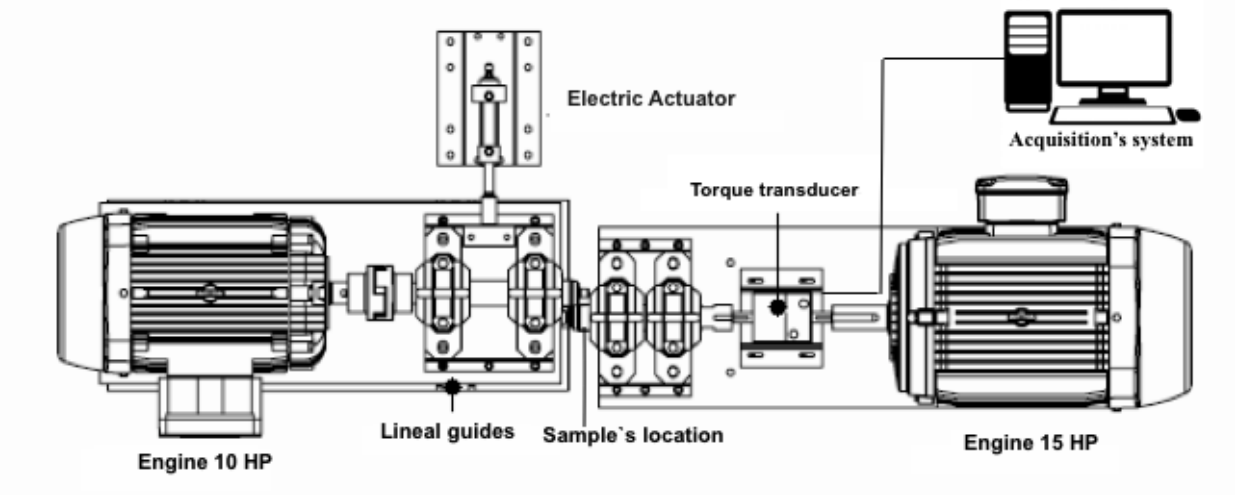

Figure 4. Schematic of the twin-disc testing machine used for all the experiments.

At the end of the tests the worn surfaces were inspected to identify the main wear mechanisms, and cross sections of the samples submitted to extreme conditions (0.8% - 7% creepage) were used for microstructure analysis and micro-hardness measurement with focus on the sub-surface deformed layer.

3. RESULTS AND DISCUSSION

3.1 Variation of COF with testing time

Figure 5 shows the variation of COF with the number of cycles for dry tests. The COF increases with the creepage reaching a stable value after 600–700 cycles approximately. For high creepages the COF is always between 0.55 and 0.60. For low creepages (0.8%) the COF value is close to 0.20. The tangential force in the stick region reaches lower values compared to those in the slip zone, therefore when the creepage increases a difference in the COF can be observed due to the increase in the size of the slip zone in the contact area. Hence, the values of the COF vary for each creepage tested [10]. For high creepages (between 3% and 7%), the value of COF decreased after 4000 cycles approximately, which has been associated to the formation of stable oxides on the surface, which act as solid lubricants [16,17].

In lubricated tests three stages are clearly observed as a function of testing time. In zone 1 (the TOR-FM has not been added yet) the COF increases until the traction force is stabilized; in zone 2 the COF decreases quickly due to the addition of the TOR-FM, and in zone 3 a constant COF value under 0.10 for all creepages is reached (Figures 6 and 7). As the addition of the TOR-FM is intermittent, the COF plots show some periodicity which is related to the actual time that the boundary layer of TOR-FM is stable on the surfaces.

3.2 Creepage and wear rate

The average COF values of the zone 3 of the curves shown in Figures 6 and 7 were used to build the Carter's curves shown in Figures 8 for dry and lubricated conditions. After 3% of creepage the COF is stabilized in the dry tests. In this case, the slip zone begins to saturate the contact area and the maximum COF is reached. Under these conditions the COF is close to 0.55, which is consistent with the literature [10,14,18] and it is in the interval for dry rail conditions reported by Stock et al [6]. In the lubricated tests (shown in detail in the top left insert in Figure 7), on the other hand, the maximum COF is reached after 5% of creepage and the maximum

value is around 0.07 for both TOR-FM's added.

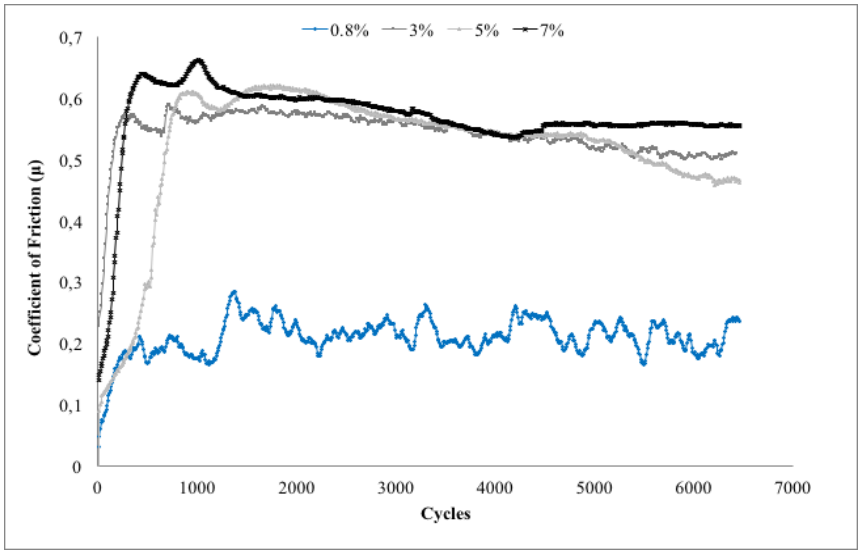

Figure 5. Coefficient of friction under dry conditions.

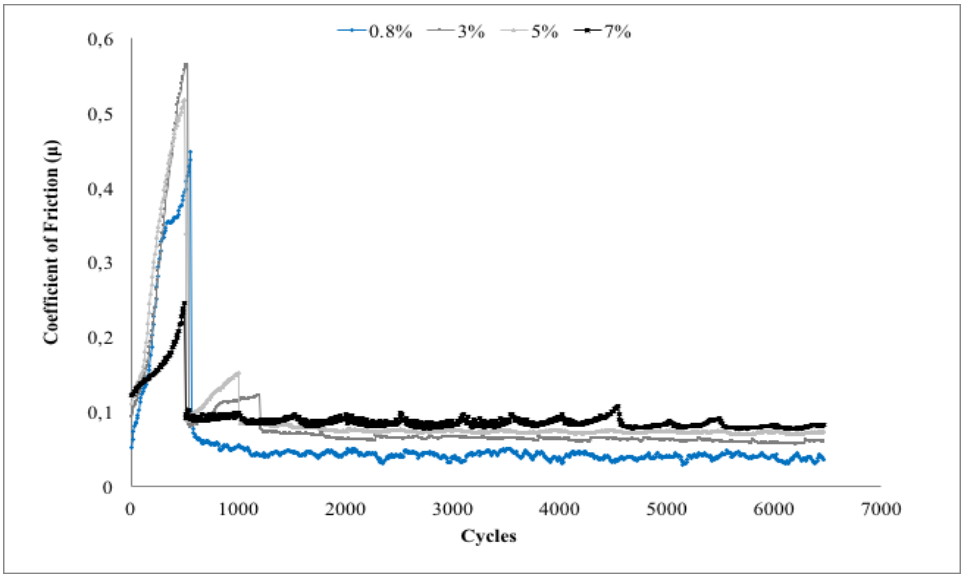

Figure 6. Coefficient of friction for tests with TOR-FM1 and different creepage values.

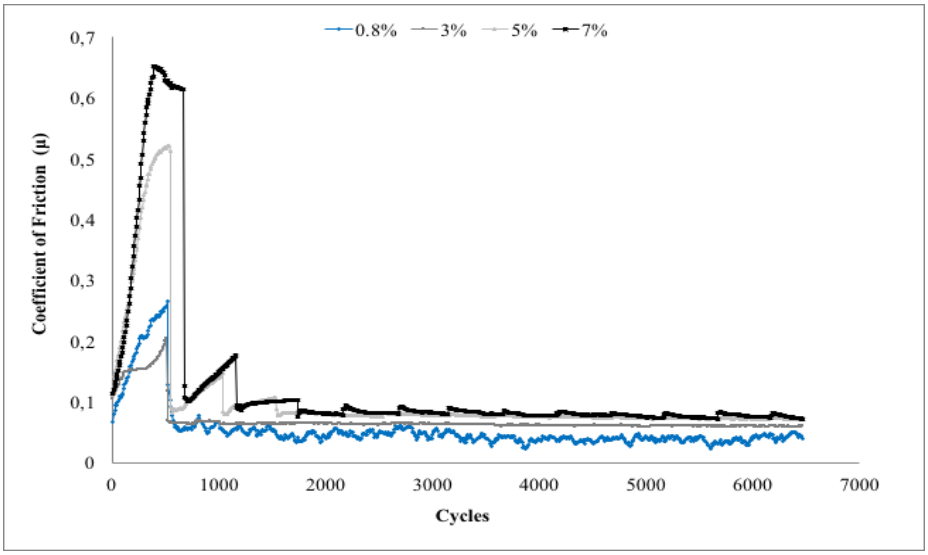

Figure 7. Coefficient of friction for tests with TOR-FM2 and different creepage values.

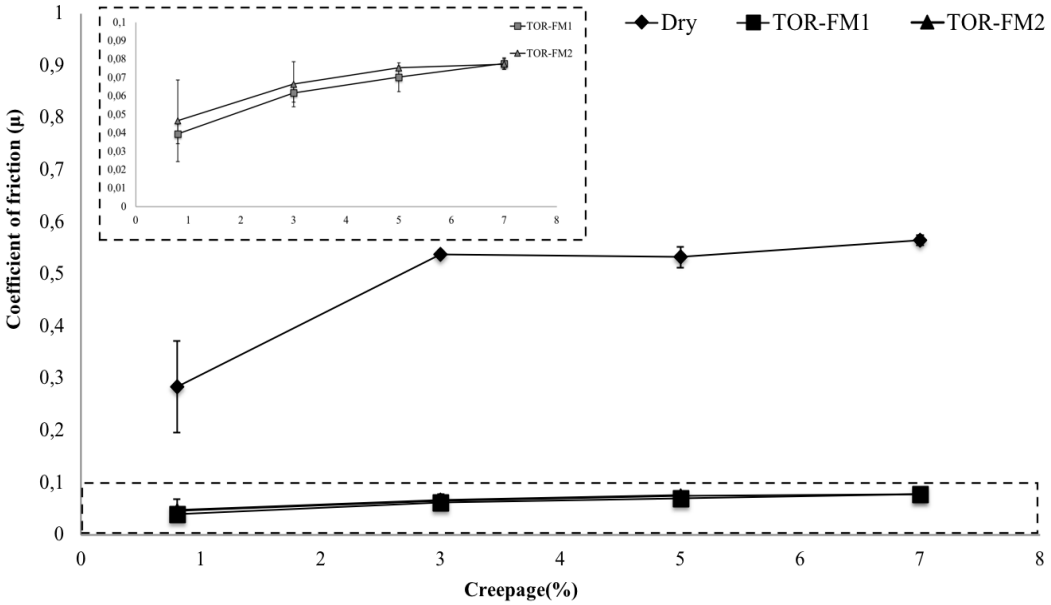

Figure 8. Creep's curves for all test conditions.

Figures 9 and 10 show the measured wear rates for rail and wheel samples as a function of creepage, together with the respective COF variation. For the wheel samples, the dry tests led to higher wear rates compared to the lubricated tests. Both rail and wheel samples tested with TOR-FM2 presented higher wear rate than those tested with TOR-FM1. This result is relevant since the COF is very similar for both TOR-FM's, which indicates that the TOR-FM's can be effective to control friction but not necessarily act the same regarding the type and intensity of the wear mechanisms responsible for surface damage. Comparing both TOR-FM's, TOR-FM2 has a lower viscosity, so a more intense crack pressurization phenomenon can be expected [19]. This is particularly relevant since during the dry stage in the lubricated tests cracks are formed. When a TOR-FM is added to the contact interface it may enter the cracks and increase its growth rate by hydrodynamic effects. In such case, the delamination process is quicker, and the wear rate is higher.

Generally speaking, the wear rate of the samples is higher when the creepage increases. In the tests with TOR-FM2, however, there is a slight decrease in wear rate when creepage increased from 5% to 7%. This occurs mainly due to an increased oxidation rate because of higher temperatures in the contact area, so the tribological pair experiences a partially-oxidative wear regime. In dry tests with large creepage values a high contact temperature is established as well, but the sub-surface volume affected by significant shear stresses is quite thicker than the oxide layers formed so the oxidative wear regime cannot be established in practice.

The results showed that the rail material has lower wear rates than the wheel material for all the conditions tested. This agrees with the typical behavior described in the literature, even when softer rails are tested [20, 21]. The difference between wear rates for rail and wheel samples is consistent with the fact that in railway systems it is much easier and cheaper replacing wheels than rails [22].

The wear rates of wheel samples under lubricated conditions were very similar regardless the TOR-FM used, with the sole exception of the tests performed with 0.8% of creepage, in which case the wear rate of wheel samples after the tests with TOR-FM2 were similar to those found in dry conditions. At this point it is worth to remind that the crack pressurization mechanism is not present in the wheel samples in a twin-disc test due to the direction of the stresses in the rolling-sliding contact with respect to the direction of crack opening [11]. Therefore, the high wear rate found in the tests with TOR-FM2 and creepage of 0.8% cannot be attributed to this mechanism. Instead, it may be a consequence of abrasive effects caused by solid-particle additives and/or wide variations in the rheological properties of the TOR-FM. This is a matter of ongoing research and no conclusive evidences can be provided currently.

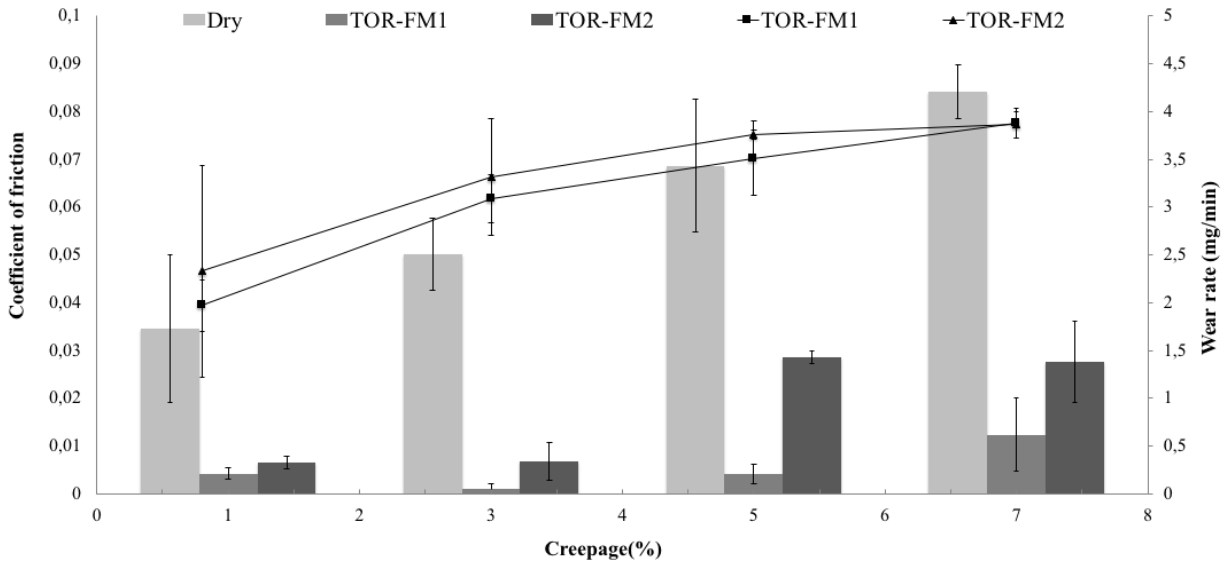

Figure 9. Wear rate of rail samples.

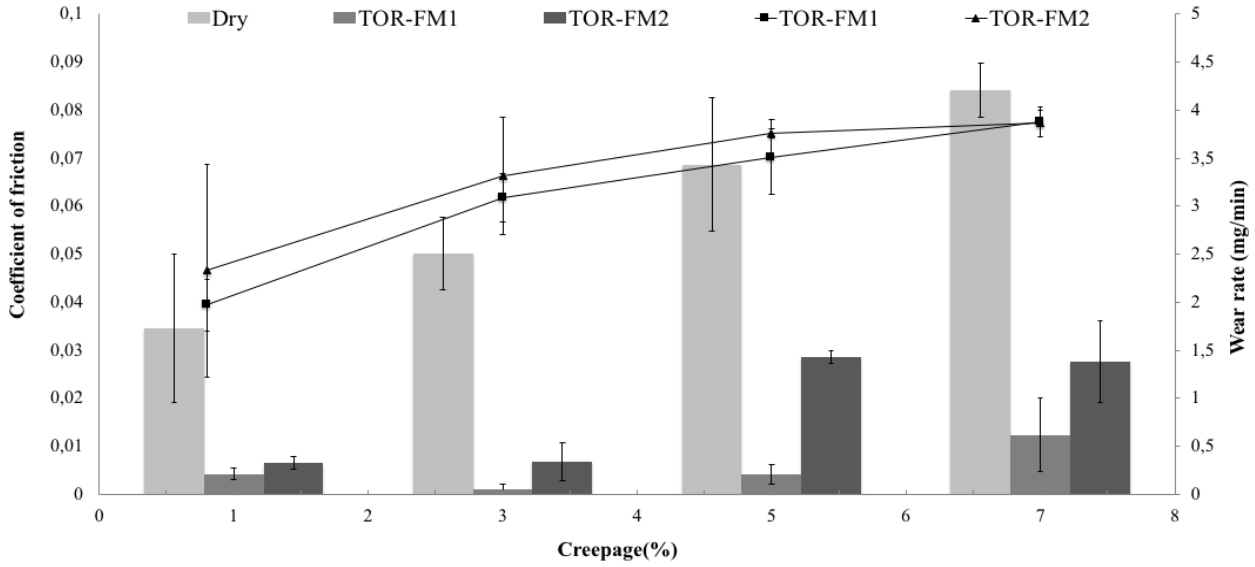

Figure 10. Wear rate of wheel samples.

3.3 Surface Analysis

Figures 11 and 12 show the aspect of the worn surfaces of rail and wheel samples respectively after tests under different lubrication conditions and creepages. Evidences of high plastic deformation in the form of ratcheting marks can be observed. Delamination is more evident for high creepages under lubricated condition (Figures 11b and 12b), which is consistent with the crack pressurization mechanism assisted by the presence of TOR-FM's in the rail samples. For low creepages the shear stresses are low, the surface damage is of less extent and in some cases machining marks can still be observed, which shows that the shear stresses imposed during the tests were of small magnitude. The presence of oxides at the surface is also evident although no homogeneous film seems to be formed.

The surface of the wheel samples shows evidences of low surface damage for the lubricated conditions with creepage of 0.8%, while for higher creepages the plastic deformation is more evident, especially in terms of delamination marks. For the dry tests, adhesion marks can be seen for 0.8% of creepage, being this the main wear mechanism. The variations of roughness parameters did not show a clear trend during the tests, mainly because the aspect of the worn surfaces does not necessarily correlate with the magnitude of the damage. This is explained by considering that the plastic deformation promotes cyclic processes of delamination and smoothing of the surface, which lead to extensive variations of the values of the roughness parameters depending on which stage (smoothing or delamination) the test is stopped.

3.4 Microstructural Analysis

Figure 13 shows cross-sectional views of the rail samples after the twin-disc tests. It can be seen that creepage has a marked influence on the plastic deformation of the samples. When creepage increases the amount of deformed sub-surface material is greater, reaching hardened depths of around 140 μm approximately under dry conditions. When the top-of-rail friction modifiers were added to the surfaces, the thickness of the deformed material was reduced to circa 50 μm. In dry testing condition the effective shear stress at the surface is much higher and it does have a considerable influence on the size of the deformed volume beneath the contact surface. Also, high tangential forces in the contact promote the crack growth in the sub-surface.

Figure 14 shows cross-sectional views of wheel samples after the tests. As in the case of the rail samples, it is evident that plastic deformation increases with creepage and decreases when a TOR-FM is applied.

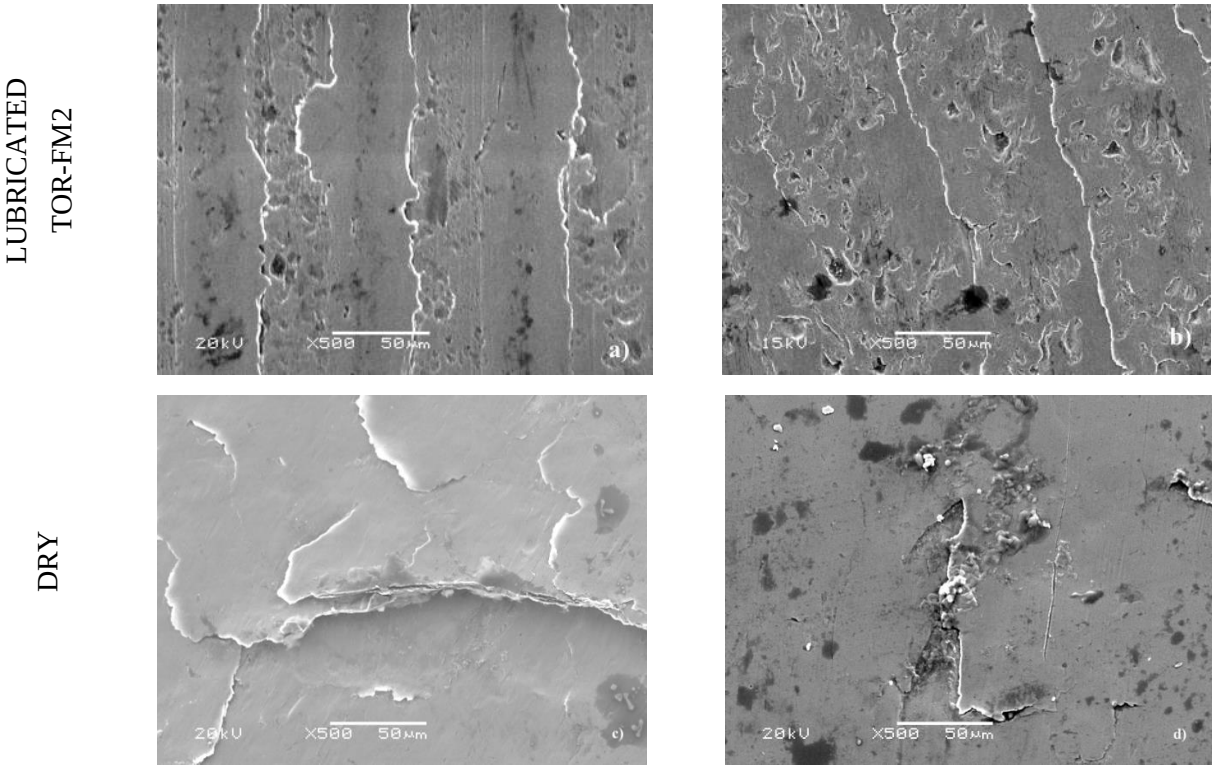

Figure 11. Surface aspect of rail samples after tests with creepage of 0.8% (left column) and 7% (right column). SEM.

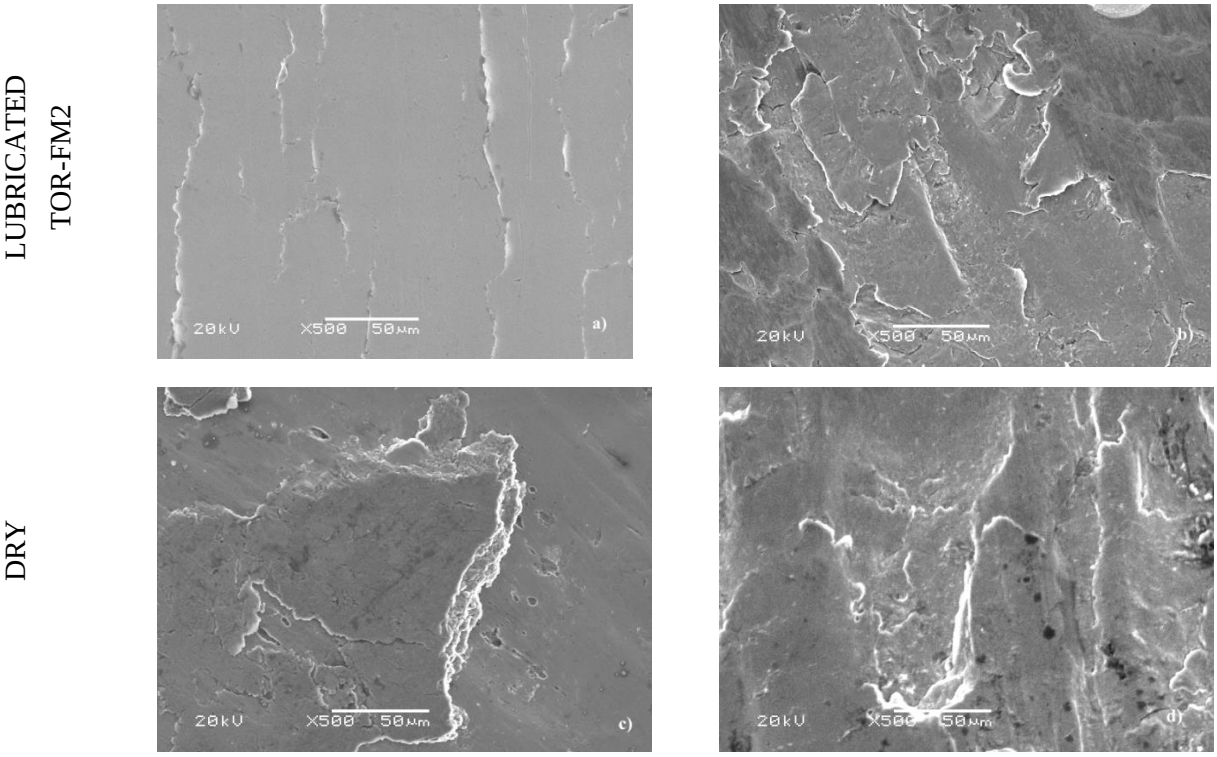

Figure 12. Surface aspect of wheel samples with creepage of 0.8% (left column) and 7% (right column). SEM.

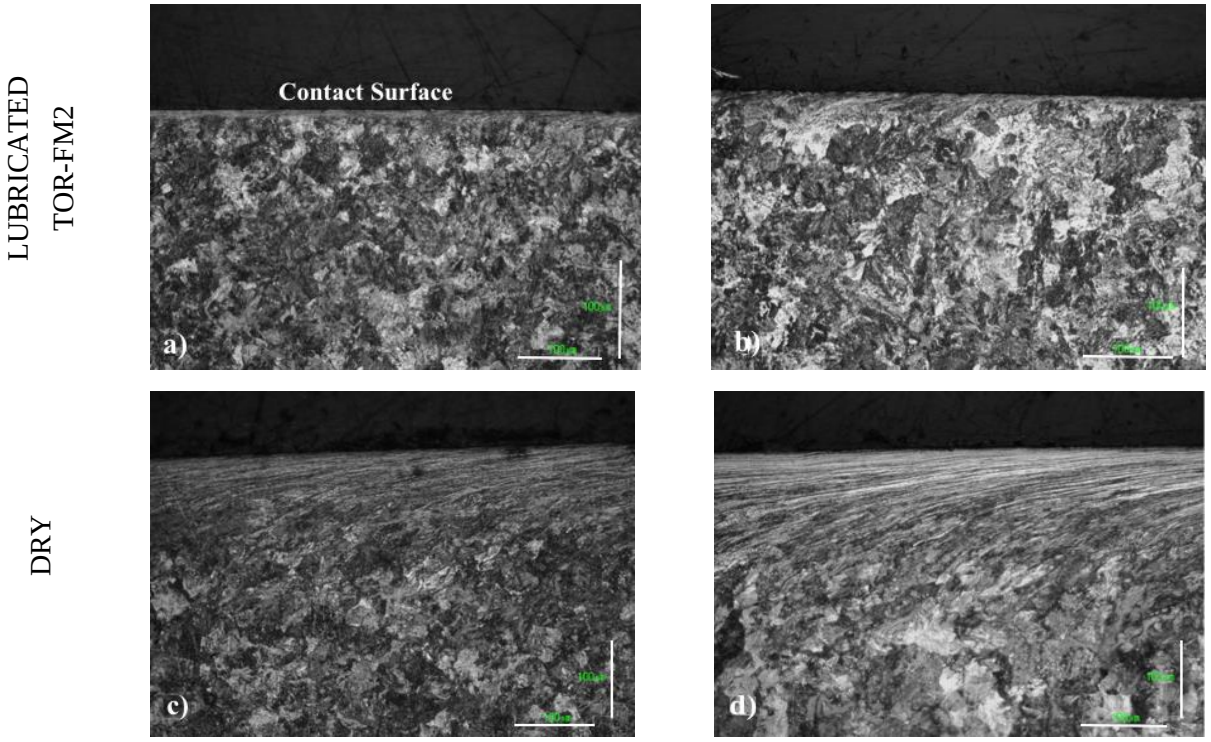

Figure 13. Cross-sectional view of the rail samples after twin-disc tests with creepage of 0.8% (left column) and 7% (right column).

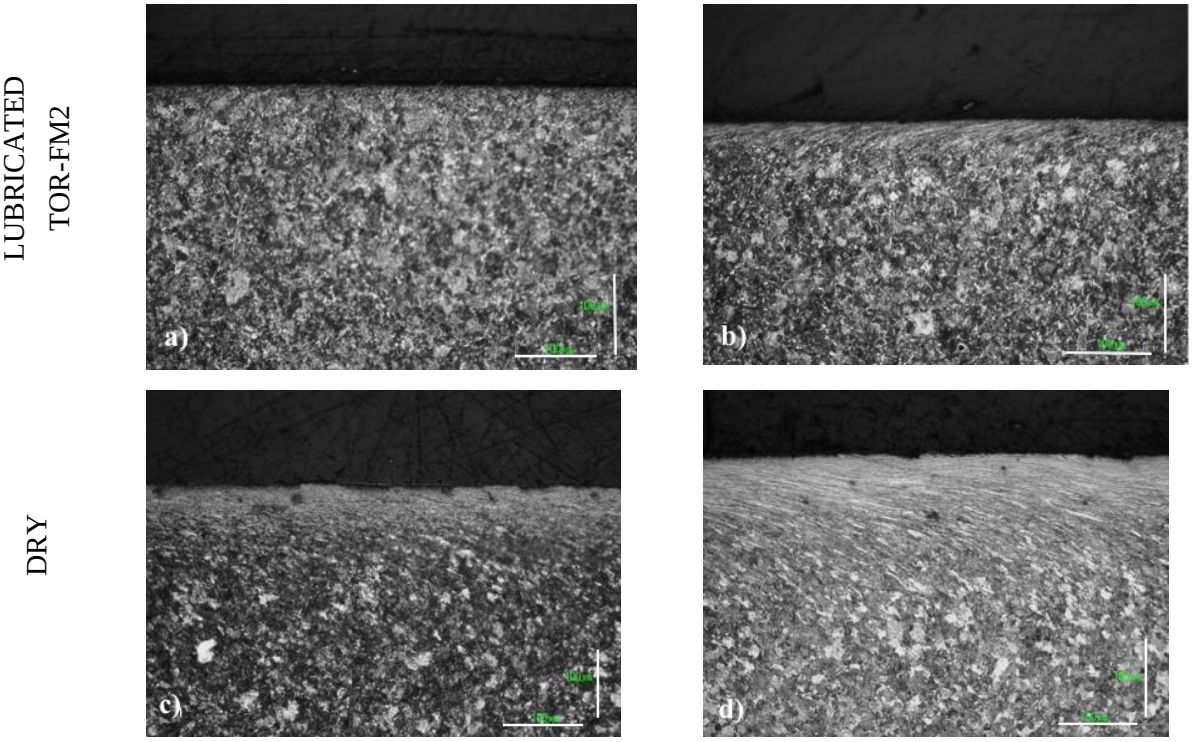

Figure 14. Cross-sectional view of the wheel samples after twin-disc tests with creepage of 0.8% (left) and 7% (right).

Figures 15 and 16 show the micro-hardness profiles of rail and wheel samples for dry (Figure 15) and lubricated (Figure 16) conditions.

Samples tested under dry conditions showed more intense hardening effects due to plastic deformation near the contact surface. The hardening effect was observed up to a depth of 200-300 µm. From this point on the hardness stabilizes around an average value similar to that of the base material. The maximum hardness values at the surface were always higher in rail samples than in wheel samples although no straightforward correlation may be drawn with creepage from the current data set.

For lubricated samples (Figure 16) the micro-hardness profiles do not show significant increases near the contact surface compared to the base material since the TOR-FM reduces the strain hardening effect caused by the traction force at the interface.

Table 3 shows a summary of the maximum values of hardness observed in the samples after the tests and the deformed layer thickness for every testing condition.

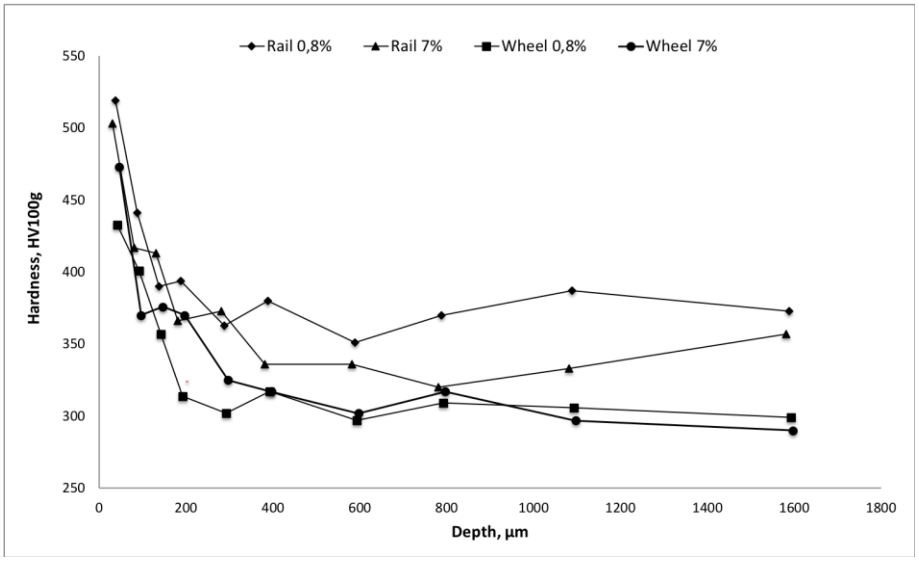

Figure 15. Micro-hardness as a function of the distance from the contact surface. Rail and wheel samples tested under dry conditions.

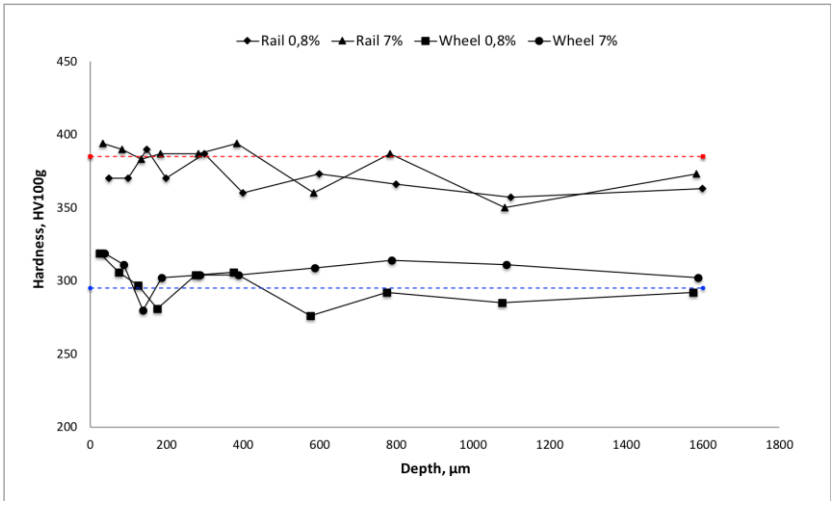

Figure 16. Micro-hardness as a function of the distance from the contact surface. Rail and wheel samples tested under lubricated conditions. The dotted lines show the average hardness of the base material.

Table 3. Maximum hardness reached after each test condition.

	Creepage 0.80%				Creepage 7%			
	Dry		Lubricated		Dry		Lubricated	
	Hardness	Depth	Hardness	Depth	Hardness	Depth	Hardness	Depth
Rail	519 HV	138 μm	390 HV	60 μm	503 HV	110 μm	394 HV	35 μm
Wheel	433HV	192 μm	319 HV	30 μm	473 HV	290 μm	319 HV	38 μm

Generally speaking, the samples tested under dry conditions systematically showed more surface damage and higher wear rate and depth of the plastically deformed region beneath the surface than those tested with the addition of friction modifiers. However, the samples tested with TOR-FM2 presented higher wear rates than those tested with TOR-FM1, which can be related in principle to the effect that the lower viscosity of the former has on the crack-pressurization mechanism: when the FM is added to the contact interface it flows into the surface defects generating a hydrostatic pressure at the tip of the cracks, which leads to a faster crack propagation.

4. CONCLUSIONS

The increase of the creepage in twin-disc tests of R350HT rail samples against ER8 wheel samples led to a significant variation of the COF in dry conditions, with maximum stable COF values between 0.5 and 0.6.

The tests performed with the addition of top of rail friction modifiers (TOR-FM1 and TOR-FM2) yielded stable COF values as low as 0.07, with reduced shear stresses at the contact surface and smaller sub-surface deformed volumes.

The samples tested with the addition of TOR-FM2 showed similar COF values than those measured with the addition of TOR-FM1, but the wear rates were dissimilar, indicating that the wear mechanisms can vary depending on the nature of the friction modified user even for equivalent friction responses.

The plastic deformation represented by ratcheting and delamination is more evident for high creepages under lubricated condition, which can be related with the crack pressurization mechanism in the rail samples in presence of the top of rail friction modifiers, especially in the case of TOR-FM2.

5. REFERENCES

[1]. Wang WJ, Lewis R, Yang B, Guo L.C, Liu QY, Zhu, "Wear and damage transition of wheel and rail materials under various contact conditions", En: Wear Vol.362-363, 2016, p. 146-152.

[2]. Jamison W, "Wear of steel in combined rolling and sliding", ASLE Transaction Vol. 25 No.1 1982, p. 71-78.

[3]. Buzelius K, "An initial investigation on the potential applicability of Acoustic emission to rail track fault detection", NDT & E international, Vol 37 No. 7, 2004, p. 507-516

[4]. Diamond S, Wolf E, "Transportation for the 21st century" TracGlide Top-of- Rail Lubrication System, Report from Department of Energy, USA, 2002

[5]. Reddy V, Chattopadhyay G, Larsson PO, Hargreaves DJ, "Modelling and analysis of Rail maintenance cost". Production Economics, Vol 105 No. 2, 2007, p. 475-482

[6]. Stock R, Stanlake L, Hardwick C, Yu M, Eadie D, Lewis R, "Material concepts for top of rail friction management – Classification, characterization and application", En: Wear Vol. 366-367, 2016, p. 225-232

[7]. Tomeoka M, Kabe N, Tanimoto M, Miyauchi E, Nakata M, "Friction control between wheel and rail by means of on-board lubrication". En: Wear Vol 253 No. 1-2, 2002, p. 124-129

[8]. Gallardo E, "Wheel and Rail Contact Simulation Using a Twin Disc Tester", PhD Thesis, Department of Mechanical Engineering, The University of Sheffield, Sheffield (England), 2008

[9]. Lewis R, Olofsson U, Wheel-rail interface handbook, CRC Press, p. 54

[10]. Johnson KL, "Contact mechanics", Cambridge University Press, 1985, p. 1-464.

[11]. Maya S, Santa JF, Toro A, "Dry and lubricated wear of rail steel under rolling contact fatigue - Wear mechanisms and crack growth", En: Wear Vol. 380-381, 2016, p. 240-250

[12]. AENOR, Norma UNE – EN 13674, "Aplicaciones ferroviarias. Vías y carriles"

[13]. AENOR, Norma UNE – EN 13362, "Aplicaciones ferroviarias. Ejes montados y bogies. Ruedas. Requisitos de producto"

[14]. Santa JF, "Development of a lubrication system for wear and friction control in wheel/rail interfaces", PhD Thesis, National University of Colombia (Colombia), 2012

[15]. Hardwick C, Lewis R, Stock R, "The effect of friction management material on rail with pre-existing rcf surface damage", En: Wear, Vol. 384-385, 2017, p. 50-60

[16]. Zhu Y, Olofsson U, Chen H, "Friction Between Wheel and Rail: A Pin On Disc Study of Environmental Conditions and Iron Oxides", En: Tribol Lett, Vol. 52, 2013, p. 327-339

[17]. Zhu Y, Chen X, Wang W, Yang H, "A study on iron oxides and surface roughness in dry and wet wheel-rail contact", En: Wear Vol. 328-329, 2015, pp. 241-248

[18]. Wang WJ, Shen P, Song JH, Guo J, Liu QY, Jin XS, "Experimental study on adhesion behavior of wheel/rail under dry and water conditions", En: Wear Vol. 27, 2011, p. 2699-2705

[19]. Hardwick C, Lewis R, Stock R, "The effects of friction management materials on rail with pre-existing RCF surface damage, En: Wear Vol. 384-385, 2017, p. 50-60

[20]. Arias-Cuevas O, Li Z, Lewis R, "A laboratory investigation on the influence of the particle size and slip during sanding on the adhesion and wear in the wheel–rail contact", En: Wear Vol. 271, 2011, p. 14-24

[21]. Arias-Cuevas O, Li Z, Lewis R, Gallardo E, "Rolling–sliding laboratory tests of friction modifiers in dry and wet wheel–rail contacts", En: Wear Vol. 268 No. 3–4, 2010, p. 543–551

[22]. Lewis R, Wang WJ, Burstow M, Lewis S, "Investigation of the Influence of Rail Hardness on the Wear of Rail and Wheel Materials under Dry Conditions", Proceedings of the Third International Conference on Railway Technology: Research, Development and Maintenance, Paper 151, Civil-Comp Press, Stirlingshire, Scotland, 2016.